Controlling the Pirouetting Motion in Rotaxanes by Counterion Exchange

Pau Farràs,*,† Eduardo C. Escudero-Adán,‡ Clara Viñas,§ and Francesc Teixidor*,§

†School of Chemistry, Newcastle University, Newcastle upon Tyne NE1 7RU, U.K.
‡Institute of Chemical Research of Catalonia (ICIQ), Avgda Països Catalans 16, 43007 Tarragona, Spain
§Institut de Ciència de Materials de Barcelona (ICMAB-CSIC), Campus de la U.A.B., E-08193 Bellaterra, Spain

Ⓢ *Supporting Information*

ABSTRACT: A fine control of the pirouetting motion of rotaxanes was achieved by using a series of metallabisdicarbollides. The latter were used as anions in the protonated form of benzylic amide macrocycle-containing fumaramide rotaxanes. The present paper discusses the synthesis and the structural and dynamic character- izations of the first examples of anionic boron cluster-containing rotaxanes. To study the dynamic properties of such molecules, the pirouetting rate of the weakly coordinating boron cluster-containing rotaxanes with the more strongly coordinating trifluoroacetate anion (TFA⁻), which would form a close ion pair with the macrocycle, was measured using the exchange spectroscopy NMR technique. Our hypothesis was that the stronger the ion pair the lower the rate of rotation due to the presence of a bigger volume of solvent to be moved. The anion would act as an anchor for the pirouetting motion. Indeed, the results show the expected trend: the rotaxane with the closely coordinating TFA⁻ anion pirouettes most slowly, and the most weakly coordinating hexabromoderivative of cobaltabisdicarbollide pirouettes the fastest.
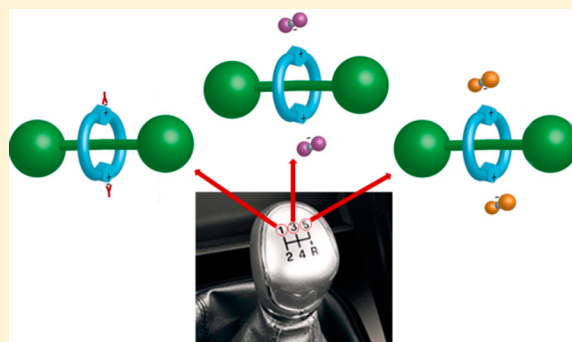
INTRODUCTION

Mechanically interlocked architectures such as rotaxanes have shown great potential for the construction of synthetic molecular machines[1,2] due to the ability of the mechanically bonded components to undergo controlled motion relative to one another, such as linear motion (shuttling[3]), rotational motion (pirouetting[4]), and pendular motion (rocking[5]). These simple systems exemplify several key principles of controlling molecular-level motion, which nature exploits to great effect in a variety of amazingly sophisticated motor proteins.[6] Large amplitude internal motion can be induced by different types of external stimuli: chemical,[7] photonic,[8] or electronic.[9] However, the control of directionality and velocity or frequency of these motions remains a challenge for the scientific community. While investigations have been carried out into many aspects of this stimulated internal motion, the pirouetting of a macrocycle relative to a thread remains a relatively unexplored topic.[10] Establishing methods for controlling aspects of such move- ments is a requisite for the development of devices that function through rotary motion. It has already been reported that the rate of pirouetting of the interlocked components of benzylic amide macrocycle-containing nitrone and fumaramide rotaxanes can be slowed down by 2 to 3 orders of magnitude by applying a modest external oscillating electric field.[11] On the other hand, an acceleration of >6 orders of magnitude can also be obtained by electronic stimuli causing isomerization of the molecule.[12]

Boron clusters are a class of inorganic structures whose chemistry is remarkable as a result of the combination of their rigidity, hydrophobicity, and chemical and thermal stability.[13] Anionic carboranes, boranes, and metallabisdicarbollides are also known to be weakly coordinating anions (WCAs).[14,15] However, some of them exhibit remarkable noncovalent interactions with surrounding molecules, and this is a promising subject of study for many applications, especially in biomedicine.[16] This combination of factors influences the reactivity of these clusters, their capacity to act as a hydrogen acceptor,[17,18] and their efficiency to occupy a given space.[19,20] These properties govern the behavior of these WCAs with counterions;[21,22] however, the exploitation of these interactions to control molecular machinery is nonexistent. Some examples can be found based on neutral *p*-carborane being used as wheels of nanocars, nanoworms, nanodragsters, etc. that exploit the interaction of the boron cluster with the surface to promote the movement of such molecular machines.[23,24] Finally, Hawthorne et al. proposed the use of metallabisdicarbollides as molecular axis to control unidirectional rotary motion.[25,26]

The present paper discusses the synthesis and the structural and dynamic characterization of the first examples of anionic boron cluster-containing rotaxanes. We will focus on the metallabisdicarbollide cobaltabisdicarbollide [3,3′-Co(1,2-

$C_2B_9H_{11})_2]^-$ [**1**]$^-$ and its hexabromoderivative [8,8′,9,9′,12,12′-Br_6-3,3′-Co(1,2-$C_2B_9H_8)_2]^-$ [**2**]$^-$, the latter being a weaker WCA due to the presence of B—Br groups on the more reactive boron vertices limiting its capacity on B—H hydrogen bonding.[27] As discussed above, the pirouetting rate of rotaxanes has previously been altered over several orders of magnitude; however, the ability to make smaller, more graduated changes has so far not been possible. We reasoned that incorporation of anionic metallabisdicarbollides in a positively charged macrocycle could be useful for fine-tuning the frequency of pirouetting through weak intermolecular interactions (Figure 1). We have previously studied the rate of pirouetting in
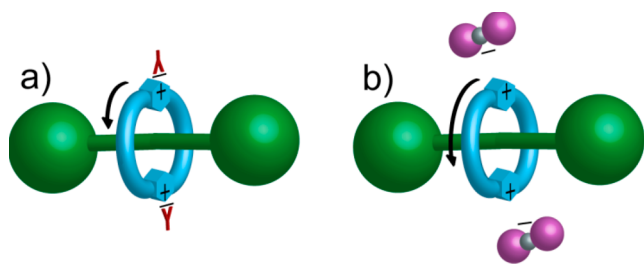

Figure 1. Controlling the rotation of the macrocycle relative to the thread (pirouetting motion) in a [2]rotaxane by counterion coordination capacity. The doubly protonated macrocycle shown in blue pirouettes more slowly with (a) a small, strongly coordinating counterion such as trifluoroacetate (shown in red) than in comparison with (b) a large, weakly coordinating counterion such as cobaltabisdicarbollide (shown in pink and gray).

rotaxanes assembled using a hydrogen bond template[28] and decided to modify the macrocycle so that it could be protonated and use different counteranions to study their effect on the pirouetting rate. Stoddart et al. demonstrated that counterion exchange could modify the dynamics in rotaxanes in a shuttling motion.[29] Therefore, we chose to compare the pirouetting rate of the weakly coordinating boron cluster-containing rotaxanes with the more strongly coordinating trifluoroacetate anion (TFA$^-$), which would form a close ion pair with the macrocycle. Our hypothesis was that the stronger the ion pair the lower the rate of rotation due to the presence of a bigger volume of solvent to be moved. The anion would act as an anchor for the pirouetting motion. Indeed, the results show the expected trend: the rotaxane with the closely coordinating TFA$^-$ anion pirouettes most slowly, and the most weakly coordinating hexabromoderivative of cobaltabisdicarbollide pirouettes the fastest.

■ EXPERIMENTAL SECTION

Instrumentation. UV−visible spectroscopy was carried out with a Shimadzu UV−vis 1700 spectrophotometer, at 22 °C, using 1 cm quartz cuvettes. ^1H NMR spectra were recorded on Bruker AV 400 instruments. The ^{11}B, $^{11}B\{^1H\}$ NMR (128.39 MHz) and $^{13}C\{^1H\}$ NMR (100.59 MHz) spectra were recorded on a Bruker Avance 400 Ultrashield spectrometer equipped with the appropriate decoupling accessories at room temperature. Chemical shift values for ^{11}B NMR and $^{11}B\{^1H\}$ spectra were referenced to external $BF_3 \cdot O(C_2H_5)_2$, and those for ^1H and $^{13}C\{^1H\}$ NMR spectra were referenced to $Si(CH_3)_4$. Chemical shifts are reported in units of parts per million downfield from reference, and all coupling constants are reported in Hertz. Standard abbreviations indicating multiplicity were used as follows: s = singlet, d = doublet, t = triplet, m = multiplet, b = broad. Fast atom bombardment (FAB) mass spectrometry (MS) was carried out by the services at the University of Edinburgh. The electrospray-ionization

mass spectra (ESI-MS) were recorded on a Bruker Esquire 3000 spectrometer using a source of ionization and an ions trap analyzer. For voltammetric determinations, an electrochemical system, VoltaLab (Universal Electrochemical Laboratory System) interfaced with a PGZ100 potentiostat (Radiometer Analytical) and controlled by the VoltaMaster 4 software, was used. The electrochemical cell contained glassy carbon electrode as working electrode, a reference Ag/AgCl/$[n(C_4H_9)_4N]Cl$ (0.1 M in CH_3CN) electrode, and platinum wire as auxiliary electrode. The solutions were deaerated with analytical grade nitrogen at the start of each experiment to prevent oxygen interference. All experiments were performed in acetonitrile with 0.1 M tetrabutylammonium hexafluorophosphate as supporting electrolyte at room temperature.

Materials. Unless stated otherwise, all reagents and solvents were purchased from Aldrich Chemicals and used without further purification. Dichloromethane, chloroform, and N,N-dimethylformamide were dried using a solvent purification system manufactured by Innovative Technology, Newburyport, MA, U.S. All reactions were carried out under an atmosphere of nitrogen. Column chromatography was carried out using Silica 60A (particle size 35−70 μm, Fisher, U.K.) as the stationary phase, and thin-layer chromatography was performed on precoated silica gel plates (0.25 mm thick, 60 F254, Merck, Germany) and observed under UV light. Cs[3,3′-Co(1,2-$C_2B_9H_{11})_2$], Cs[**1**], was obtained from Katchem and protonated using 3 × 25 mL of an aqueous 1 M HCl solution. Cs[8,8′,9,9′,12,12′-Br_6-3,3′-Co(1,2-$C_2B_9H_8)_2$], Cs[**2**], was synthesized according to the literature[30] and protonated using 3 × HCl (1 M). [8-($OCH_2CH_2)_2$-3,3′-Co(1,2-$C_2B_9H_{10})(1′,2′-C_2B_9H_{11})$], [**9**], was prepared according to the literature.[31]

Synthesis of N,N,N,N-Tetraisooctylfumaramide, [3]. Fumaryl chloride (0.52 mL, 4.85 mmol in $CHCl_3$, 5 mL) was added dropwise to a stirred solution of diisooctylamine (3.2 mL, 10.6 mmol) and Et_3N (1.48 mL, 10.6 mmol) in $CHCl_3$ (50 mL) at 0 °C under an atmosphere of nitrogen. The reaction was stirred at 0 °C for a further 2 h. The solution was then washed twice with 10 mL of a 1 M aqueous HCl solution, twice with 10 mL saturated aqueous $NaHCO_3$ solution, twice with a saturated aqueous NaCl solution, dried ($MgSO_4$), and concentrated under reduced pressure. This material was purified by flash chromatography (SiO_2: methanol/chloroform, 0:100 to 3:97) to provide thread [**3**] as a yellowish oil. Yield: 2.05 g (75%). ^1H NMR (400 MHz, $CDCl_3$): δ = 7.42 (s, 2H, H_e), 3.35 (m, 8H, H_d, and $H_{d′}$), 1.73 (q, 2H, J = 5.6, H_c), 1.60 (q, 2H, J = 7.2, $H_{c′}$), 1.28 (m, 32H, H_b), 0.89 (m, 24H, H_a).

Synthesis of Rotaxane, E-[4]. Thread [**3**] (281 mg, 0.50 mmol) was dissolved in anhydrous $CHCl_3$ (50 mL) and stirred vigorously, while solutions of p-xylylene diamine (539 mg, 3.96 mmol) and Et_3N (1.2 mL, 3.96 mmol) in anhydrous $CHCl_3$ (20 mL) and pyridine-3,5-dicarbonyl dichloride (810 mg, 3.96 mmol) in anhydrous $CHCl_3$ (20 mL) were simultaneously added over a period of 4 h using motor-driven syringe pumps. After a further 16 h the resulting suspension was filtered and concentrated under reduced pressure. This material was purified by flash chromatography (SiO_2: methanol/dichloromethane, 4:96) to provide rotaxane [**4**] as a colorless solid. Yield: 43 mg (8%). ^1H NMR (400 MHz, $CDCl_3$): δ = 9.41 (s, 4H, H_A), 9.04 (s, 2H, H_B), 7.46 (m, 4H, H_C), 7.00 (s, 8H, H_D), 5.94 (s, 2H, H_e), 5.09 (m, 4H, H_{E1}), 3.81 (m, 4H, H_{E2}), 3.14 (m, 4H, H_d), 2.91 (m, 4H, $H_{d′}$), 1.57 (m, 4H, H_c), 1.19 (m, 32H, H_b), 0.77 (m, 24H, H_a); $^{13}C\{^1H\}$ NMR (100 MHz, $CDCl_3$): δ = 166.3, 164.0, 153.2, 137.6, 130.4, 129.3, 127.8, 54.2, 52.6, 43.9, 39.0, 38.6, 28.7, 27.7, 22.9, 13.9, 10.2; high-resolution (HR) ESI-MS-pos: m/z = 1097.7496 (calc. for $C_{66}H_{96}O_6N_8$ 1097.7526).

Protonation of Rotaxane [4] with CF₃COOH, E-[5]. Rotaxane [**4**] (10 mg, 9.1 μmol) was dissolved in dichloromethane (2 mL), and trifluoroacetic acid (3 μL, 30 μmol) was added. After stirring for 10 min it was concentrated under reduced pressure. Yield: 12 mg (99%). ^1H NMR (400 MHz, CD_3CN): δ = 9.83 (s, 2H, H_B), 9.36 (s, 4H, H_A), 7.85 (m, 4H, H_C), 7.12 (s, 8H, H_D), 5.96 (s, 2H, H_e), 4.99 (m, 4H, H_{E1}), 4.13 (m, 4H, H_{E2}), 3.40−3.02 (m, 8H, H_d and $H_{d′}$), 1.64 (br s, 2H, H_c), 1.43 (br s, 2H, $H_{c′}$), 1.22 (m, 32H, H_b), 0.84 (m, 24H, H_a); $^{13}C\{^1H\}$ NMR (100 MHz, $CDCl_3$): δ = 166.7, 164.0, 153.6, 137.4,

8655

dx.doi.org/10.1021/ic501246e | Inorg. Chem. 2014, 53, 8654−8661

129.3, 118.7, 49.5, 38.7, 29.5, 27.8, 23.1, 14.0, 10.6; HRESI-MS-pos: m/z = 1119.7342 (calc. for $C_{66}H_{96}O_6N_8Na$ 1119.7345); HRESI-MS-neg: m/z = 248.9605 (calc. for $C_4F_6O_4Na$ 248.9604).

Protonation of Rotaxane [4] with H[3,3′-Co(1,2-C₂B₉H₁₁)₂], E-[6]. Rotaxane [**4**] (10 mg, 9.9 μmol) was dissolved in dichloromethane (2 mL), and a solution of H[**1**] (9.6 mg, 30 μmol) in dichloromethane (2 mL) was added slowly. The orange solution is concentrated under reduced pressure. The remaining solid was washed with Et₂O to remove the excess of H[**1**]. Yield: 16 mg (99%). ¹H NMR (400 MHz, CD₃CN): δ = 9.73 (s, 2H, H$_B$), 9.17 (s, 4H, H$_A$), 7.55 (m, 4H, H$_C$), 7.00 (s, 8H, H$_D$), 5.82 (s, 2H, H$_e$), 4.74 (br s, 4H, H$_{E1}$), 4.03, 4.00 (br s, 2H, H$_f$), 3.90 (m, 4H, H$_{E2}$), 3.66 (br s, 6H, H$_f$), 3.10 (m, 4H, H$_d$), 2.90 (m, 4H, H$_{d′}$), 1.43 (m, 2H, H$_c$), 1.20 (m, 2H, H$_{c′}$), 1.12−0.83 (m, 32H, H$_b$), 0.63−0.48 (m, 24H, H$_a$); ¹³C{¹H} NMR (100 MHz, CD₃CN): δ = 166.2, 162.7, 149.9, 136.6, 133.4, 129.2, 128.9, 53.8, 52.4, 51.1, 49.3, 43.7, 38.4, 30.4, 29.4, 28.4, 27.3, 23.8, 22.6, 13.5, 9.9, 9.6; ¹¹B NMR (128 MHz, CD₃CN): δ = 6.08 (d, 2B, J = 164), 1.02 (d, 2B, J = 140), −5.80 (d, 4B, J = 109), −6.54 (d, 4B, J = 141), −17.68 (d, 4B, J = 164), −23.13 (d, 2B, J = 164); HRESI-MS-pos: m/z = 1119.7331 (calc. for $C_{66}H_{96}O_6N_8Na$ 1119.7345); HRESI-MS-neg: m/z = 324.2851 (calc. for $C_4H_{22}B_{18}Co$ 324.2846).

Protonation of Rotaxane [4] with H[8,8′,9,9′,12,12′-Br₆-3,3′-Co(1,2-C₂B₉H₈)₂], E-[7]. Rotaxane [**4**] (10 mg, 9.9 μmol) was dissolved in dichloromethane (2 mL), and an excess of a H[**2**] solution in dichloromethane was added. The orange solution is concentrated under reduced pressure. The remaining solid was washed with Et₂O to remove the excess of H[**2**]. Yield: 24 mg (99%). ¹H NMR (400 MHz, CD₃CN): δ = 9.76 (s, 2H, H$_B$), 9.20 (s, 4H, H$_A$), 7.58 (m, 4H, H$_C$), 7.03 (s, 8H, H$_D$), 5.85 (s, 2H, H$_e$), 4.89 (br s, 1H, H$_f$), 4.77 (m, 4H, H$_{E1}$), 4.63 (br s, 1H, H$_f$), 4.49 (br s, 6H, H$_f$), 3.93 (m, 4H, H$_{E2}$), 3.15−2.82 (m, 8H, H$_{d/d′}$), 1.46 (br s, 2H, H$_c$), 1.23 (br s, 2H, H$_{c′}$), 1.04−0.98 (m, 32H, H$_b$), 0.66−0.51 (m, 24H, H$_a$); ¹³C{¹H} NMR (100 MHz, CDCl₃): δ = 167.2, 163.7, 148.9, 137.9, 130.4, 55.2, 53.2, 44.8, 39.9, 31.3, 30.4, 29.2, 28.3, 23.5, 14.2, 10.3; ¹¹B NMR (128 MHz, CD₃CN): δ = 5.21 (s, 2B, B8, B8′), 3.20 (d, 2B, J = 178), −2.33 (s, 4B, B9, B9′, B12, B12′), −5.11 (d, 4B, J = 150), −17.65 (d, 4B, J = 159), −24.02 (d, 2B, J = 173); HRESI-MS-pos: m/z = 1097.7540 (calc. for $C_{66}H_{97}O_6N_8$ 1097.7526); HRESI-MS-neg: m/z = 796.7424 (calc. for $C_4H_{16}B_{18}Br_6Co$ 796.7448).

Synthesis of N,N-Diisooctylfumaramide, E-[8]. Fumaryl chloride (0.52 mL, 4.85 mmol in CHCl₃, 5 mL) was added dropwise to a stirred solution of 2-ethylhexylamine (1.8 mL, 10.6 mmol) and Et₃N (1.48 mL, 10.6 mmol) in CHCl₃ (50 mL) at 0 °C under an atmosphere of nitrogen. The reaction was stirred at 0 °C for a further 2 h. The solution was then washed twice with 10 mL of a 1 M aqueous HCl solution, twice with 10 mL of a saturated aqueous NaHCO₃ solution, twice with 10 mL of a saturated aqueous NaCl solution, dried (MgSO₄), and concentrated under reduced pressure. This material was purified by flash chromatography (SiO₂: methanol/chloroform, 3:97) to provide thread [**8**] as a yellowish oil (0.69 g, 42%). ¹H NMR (400 MHz, CDCl₃): δ = 6.90 (s, 2H, H$_e$), 6.16 (br s, 2H, NH), 3.23 (m, 4H, H$_d$), 1.44 (m, 2H, H$_c$), 1.21 (m, 16H, H$_b$), 0.83 (m, 12H, H$_a$).

Synthesis of Potassium N,N-{8-(1,3-Dioxohexane)-3,3′-Co(1,2-C₂B₉H₁₀)(1′,2′-C₂B₉H₁₁)}-N,N-diisooctylfumaramide, E-[10]. A solution of thread [**8**] (0.31 g, 0.90 mmol) in toluene (10 mL) was added at 0 °C to a stirred solution of sodium hydride (0.15 g, 3.6 mmol) in tetrahydrofuran (20 mL). The reaction was stirred at 0 °C for a further 2 h. Then, a solution of [**9**] (0.73 g, 1.8 mmol) was slowly added at 0 °C and left overnight. The solution was concentrated under reduced pressure. The residue was then washed three times with 20 mL of a 1 M aqueous HCl solution, three times with 20 mL of a saturated aqueous KHCO₃ solution, dried (MgSO₄), and concentrated under reduced pressure. This material was purified by flash chromatography (SiO₂: acetonitrile/dichloromethane, 30:70) to provide thread [**10**] as an orange solid. Yield: 1.00 g (90%). ¹H NMR (400 MHz, CD₃CN): δ = 7.25 (s, 2H, H$_e$), 4.23, 4.18, 4.16, 4.11 (br s, 8H, H$_i$), 3.64 (t, 4H, J = 5, H$_h$), 3.59 (m, 8H, H$_g$ and H$_f$), 3.49 (t, 4H, J = 5, H$_{d′}$), 3.38 (d, 4H, J = 7, H$_d$), 1.66 (br s, 2H, H$_c$), 1.30 (m, 16H, H$_b$), 0.91 (m, 12H, H$_a$); ¹³C{¹H} NMR (100 MHz, CD₃CN): δ = 166.0, 131.4, 72.0, 69.4, 68.7, 53.3, 52.3, 49.5, 46.8, 38.9, 37.2, 30.3, 28.4, 23.6, 22.8, 17.5, 13.4, 10.2;

¹¹B NMR (128 MHz, CD₃CN): δ = 23.32 (s, 2B, B8), 4.32 (d, 2B, J = 128), 0.03 (d, 2B, J = 134), −2.71 (d, 2B, J = 134), −4.74 (d, 2B, J = 140), −7.73 (d, 16B), −17.53 (d, 4B, J = 145), −20.39 (d, 4B, J = 150), −22.16 (d, 2B, J = 184), −28.90 (d, 2B, J = 150); FAB-MS: m/z (%): 428.6 (M-C₃₂H₇₃B₁₈N₂O₆Co, 100), 579.8 (M, 58).

Synthesis of Rotaxane, E-[11]. Thread [**10**] (612 mg, 0.50 mmol) was dissolved in anhydrous CHCl₃ (50 mL) and stirred vigorously, while solutions of *p*-xylylene diamine (540 mg, 3.96 mmol) and Et₃N (1.1 mL, 3.96 mmol) in anhydrous CHCl₃ (20 mL) and pyridine-3,5-dicarbonyl dichloride (810 mg, 3.96 mmol) in anhydrous CHCl₃ (20 mL) were simultaneously added over a period of 4 h using a motor-driven syringe pumps. After a further 16 h the resulting suspension was filtered and concentrated under reduced pressure. The residue was then washed three times with 20 mL of a 1 M aqueous HCl solution, dried (MgSO₄), and concentrated under reduced pressure. This material was purified by flash chromatography (SiO₂: ethyl acetate/acetonitrile, 90:10 to 70:30) to provide rotaxane [**11**] as an orange solid. Yield: 148 mg (18%). ¹H NMR (400 MHz, CD₃CN): δ = 9.32 (s, 4H, H$_A$), 9.20 (s, 2H, H$_B$), 7.65 (m, 4H, H$_C$), 7.15 (s, 8H, H$_D$), 6.00 (d, 2H, J = 22, H$_e$), 5.10 (m, 4H, H$_{E1}$), 4.20, 4.13 (br s, 8H, H$_i$), 3.64 (t, 4H, J = 5, H$_h$), 3.59 (m, 8H, H$_g$ and H$_f$), 3.54 (m, 4H, H$_{d′}$), 3.38 (d, 4H, J = 5, H$_d$), 1.69, 1.45 (br s, 2H, H$_c$), 1.24 (m, 16H, H$_b$), 0.85 (m, 12H, H$_a$). ¹³C{¹H} NMR (100 MHz, CD₃CN): δ = 166.1, 164.9, 151.9, 144.1, 130.9, 129.4, 128.9, 72.0, 68.4, 67.9, 53.9, 46.7, 43.1, 37.9, 29.7, 29.0, 28.5, 27.8, 22.8, 22.6, 13.4, 13.3, 9.8; ¹¹B NMR (128 MHz, CD₃CN): δ = 23.40 (s, 2B, B8), 4.32 (d, 2B, J = 137), 0.03 (d, 2B, J = 132), −2.79 (d, 2B, J = 146), −4.83 (d, 2B, J = 128), −7.73 (d, 16B), −17.56 (d, 4B, J = 175), −20.56 (d, 4B, J = 151), −22.31 (d, 2B, J = 190), −28.75 (d, 2B, J = 130); FAB-MS: m/z (%): 846.6 (M, 100), 578.9 (M-C₃₀H₂₈O₄N₆, 25%); HRESI-MS-neg: m/z = 1716.1298 (calc. for $C_{66}H_{120}B_{36}Co_2N_8O_{10}Na$ 1716.1270).

Synthesis of Rotaxane, Z-[4]. Rotaxane E-[**4**] (80 mg, 0.07 mmol) was dissolved in dichloromethane and irradiated for 15 min in a 312 nm photoreactor. The solution was concentrated under reduced pressure. This material was purified by flash chromatography (SiO₂: methanol/dichloromethane, 5:95) to provide rotaxane Z-[**4**] as a colorless solid. The remaining trans isomer was irradiated again for 15 min, and the material was purified with the same column. Yield: 44.9 mg (56%). ¹H NMR (400 MHz, CDCl₃): δ = 9.18 (s, 4H, H$_A$), 8.19 (s, 2H, H$_B$), 7.50 (m, 4H, H$_C$), 7.18 (s, 8H, H$_D$), 4.82 (s, 2H, H$_e$), 4.47 (m, 8H, H$_E$), 2.82−2.56 (m, 8H, H$_d$), 1.51 (m, 4H, H$_c$), 1.04 (m, 32H, H$_b$), 0.78−0.68 (m, 24H, H$_a$).

Protonation of Rotaxane Z-[4] with CF₃COOH, Z-[5]. Rotaxane Z-[**4**] (11 mg, 10 μmol) was dissolved in dichloromethane (2 mL), and trifluoroacetic acid (3 μL, 30 μmol) was added. After stirring for 10 min it was concentrated under reduced pressure. Yield: 11 mg (98%). ¹H NMR (400 MHz, CDCl₃): δ = 9.30 (s, 4H, H$_A$), 8.73 (s, 2H, H$_B$), 8.19 (m, 4H, H$_C$), 7.22 (s, 8H, H$_D$), 4.85 (s, 2H, H$_e$), 4.46 (m, 8H, H$_E$), 2.91−2.76 (m, 8H, H$_d$), 1.53 (m, 4H, H$_c$), 1.06 (m, 32H, H$_b$), 0.84−0.67 (m, 24H, H$_a$).

Protonation of Rotaxane Z-[4] with H[3,3′-Co(1,2-C₂B₉H₁₁)₂], Z-[6]. Rotaxane Z-[**4**] (11 mg, 10 μmol) was dissolved in dichloromethane (2 mL), and an excess of a H[**1**] solution in dichloromethane was added. The orange solution was concentrated under reduced pressure. The remaining solid was washed with Et₂O to remove the excess of H[**1**]. Yield: 15 mg (98%). ¹H NMR (400 MHz, CD₃CN): δ = 9.12 (s, 4H, H$_A$), 8.13 (s, 2H, H$_B$), 7.90 (m, 4H, H$_C$), 7.44 (s, 8H, H$_D$), 5.31 (s, 2H, H$_e$), 4.51 (m, 8H, H$_E$), 4.45, 4.35 (br s, 2H, H$_f$), 4.25, 4.22 (br s, 6H, H$_f$), 3.10 (m, 8H, H$_d$), 1.49 (m, 4H, H$_c$), 1.24 (m, 32H, H$_b$), 0.95−0.69 (m, 24H, H$_a$).

Protonation of Rotaxane Z-[4] with H[8,8′,9,9′,12,12′-Br₆-3,3′-Co(1,2-C₂B₉H₈)₂], Z-[7]. Rotaxane Z-[**4**] (11 mg, 10 μmol) was dissolved in dichloromethane (2 mL), and an excess of a H[**2**] solution in dichloromethane was added. The orange solution is concentrated under reduced pressure. The remaining solid was washed with Et₂O the remove the excess of H[**2**]. Yield: 24 mg (99%). ¹H NMR (400 MHz, CD₃CN): δ = 9.20 (s, 2H, H$_B$), 9.06 (s, 4H, H$_A$), 8.54 (m, 4H, H$_C$), 7.28 (s, 8H, H$_D$), 4.86 (s, 2H, H$_e$), 4.98, 4.72 (br s, 2H, H$_f$), 4.58 (br s, 6H, H$_f$), 4.38 (m, 8H, H$_E$), 3.10 (m, 8H, H$_d$), 1.50 (m, 4H, H$_c$), 1.30−1.10 (m, 32H, H$_b$), 0.80−0.60 (m, 24H, H$_a$).

X-ray Crystal Structure Determination. Crystals complex *E*-[**4**] was obtained by slow diffusion of hexane in a dimethyl sulfoxide solution. The measured crystals were prepared under inert conditions immersed in perfluoropolyether as a protecting oil for manipulation.

Data Collection. Crystal structure determinations were carried out by using a Bruker-Nonius diffractometer equipped with an APPEX 2 4K CCD area detector, a FR591 rotating anode with Mo Kα radiation, Montel mirrors as the monochromator, and an Oxford Cryosystem plus low-temperature device (*T* = −173 °C). Full-sphere data collection was used with ω and ϕ scans. Programs used: Data collection APPEX-2,[32] data reduction Bruker Saint[33] V/.60A.
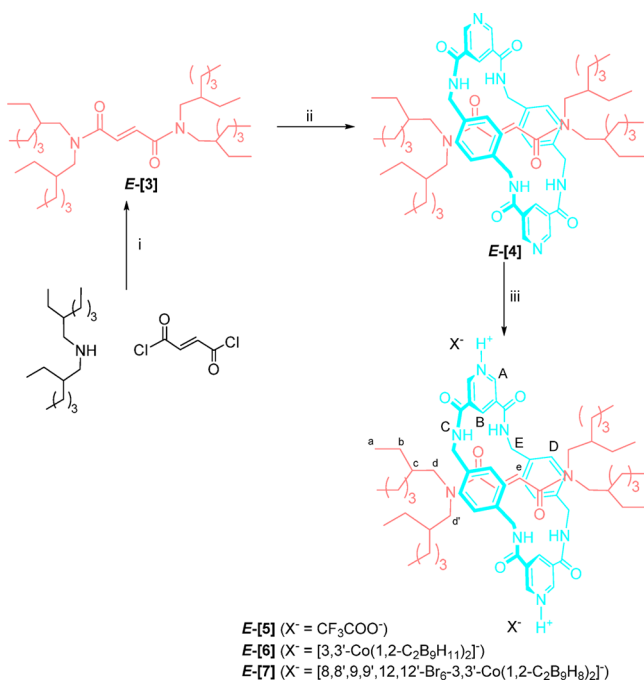
Structure Solution and Refinement. Crystal structure solution was achieved by using direct methods as implemented in SHELXTL[34] and visualized by using the program XP. Missing atoms were subsequently located from difference Fourier synthesis and added to the atom list. Least-squares refinement on F^2 by using all measured intensities was carried out with the program SHELXTL. All non-hydrogen atoms were refined, including anisotropic displacement parameters. The structure was deposited at the CCDC with reference number 1004411.

This sample was measured using Cu radiation, and the sample turned out to be a combination of two crystals with a 56:44 occupancy ratio. For the absorption correction TWINABS was used.[35] For the resolution SIR 2011 was used.[36]

■ RESULTS AND DISCUSSION

Synthesis of Rotaxanes. Fumaramide *E*-[**3**], the axle precursor of rotaxane *E*-[**4**], was obtained by reaction of diisooctylamine and fumaryl chloride as shown in Scheme 1. Subsequent formation of rotaxane *E*-[**4**] was accomplished via a five-component hydrogen bond templated clipping reaction[37] in which the fumaramide template guides the reaction between isophthaloyl dichloride and *para*-xylylenediamine. Bulky amide

Scheme 1. Hydrogen Bond Templated Synthesis of Rotaxanes with a Doubly Positively Charged Macrocycle with a Range of Counterions[a]


E-[**3**]

E-[**4**]

E-[**5**] (X⁻ = CF₃COO⁻)
E-[**6**] (X⁻ = [3,3'-Co(1,2-C₂B₉H₁₁)₂]⁻)
E-[**7**] (X⁻ = [8,8',9,9',12,12'-Br₆-3,3'-Co(1,2-C₂B₉H₈)₂]⁻)

[a]Reagents and conditions: (i) Et₃N, CHCl₃, 0 °C, 2 h (75% yield). (ii) *Para*-xylene diamine, pyridine-3,5-dicarbonyl dichloride, Et₃N, CHCl₃, rt, 20 h (8% yield). (iii) Trifluoroacetic acid or H[**1**] or H[**2**], CH₂Cl₂ (quantitative yield).

substituents are required to prevent dissociation of the macrocycle from the thread by slipping; we found that a previously reported[38] branched alkyl chain stopper served this purpose while also imparting good solubility.[39] The protonation of the two pyridine groups on the macrocycle of rotaxane *E*-[**4**] with trifluoroacetic acid led to *E*-[**5**]. The reaction of trifluoroacetic acid with H[**1**] yielded *E*-[**6**], whereas that reaction with H[**2**] led to *E*-[**7**].

In addition to the rotaxanes with varying discrete counterions, zwitterionic rotaxane *E*-[**11**] with bulky cobaltabisdicarbollide stoppering groups was synthesized (Scheme 2) to allow investigations into the effect of a "tethered" intramolecular counterion. First, secondary amide thread *E*-[**8**] was prepared, and subsequent nucleophilic attack by the in situ-prepared anion on cyclic oxonium [**9**] yielded dianionic thread *E*-[**10**] with "tethered" cobaltacarborane units. A hydrogen bond templated clipping rotaxane forming reaction followed by protonation of the pyridine moieties furnished rotaxane *E*-[**11**]. There are many examples of ionic templated rotaxanes where either thread or macrocycle are positively charged and the counteranion is not covalently bonded to neither of them.[40,41] On the other hand, there are fewer examples where an anionic stopper is used to compensate the positive charge on the axle as it is advantageous if they want to be incorporated into solid-state devices.[42,43] Finally, zwitterionic rotaxanes where the positive charge is located on the macrocycle and the negative charge is located on the thread (without being on the stoppers) can also be found. There, the charged moiety is used to template the formation or locking of the macrocycle inside the thread.[44,45] Remarkably, rotaxane *E*-[**11**] in its protonated form represents a rare example of zwitterionic rotaxane in which charges are located on different components; the negative charges are located on the bulky stoppers at the thread, and the positive charges are located on the macrocycle. We were interested on the influence of the distance between charges on the dynamics of pirouetting rate.

NMR Spectra Considerations. The formation of rotaxanes *E*-[**5**]−[**7**] and *E*-[**11**] was established unambiguously by ¹H NMR, ¹¹B NMR, ¹³C{¹H} NMR, and HRESI-MS, and characteristic upfield shifts of the fumaramide double bond proton resonances in comparison with the thread precursors as a result of interlocking were observed in the ¹H NMR spectra. Comparison of the ¹H NMR spectra of rotaxanes *E*-[**5**]−[**7**] indicates that the chemical environment experienced by thread and macrocycle protons is essentially the same in the presence of a closely coordinating counterion (Figure 2a) or a WCA (Figure 2b,c). Unexpectedly, the eight C_C−H (C_C = cage carbon) resonances of the C_{2v} symmetric cobaltabisdicarbollide counterions of rotaxane *E*-[**6**] do not appear as a singlet, instead appearing as three resonances with intensities of 1:1:6 (Figure 2d). Our hypothesis is that even though metal-labisdicarbollides are considered to be weakly coordinating anions they still can interact through the carbon cluster C_c−H groups;[46] one hydrogen atom of each cobaltacarborane fragment interacts with an atom with a lone electron pair, most probably from the macrocycle. However, this interaction is weak as can be seen by the low-field shift in the ¹H NMR spectrum. In contrast, *E*-[**7**] has a singlet corresponding to eight C_c−H resonances. The low-field shift in this molecule is higher than the previous one due to a stronger interaction of the C_c−H vertices in each C_2B_3 unit with the bromine atom of the B(8)−Br at the other dicarbollide cage. The strong

Scheme 2. Synthesis of a Zwitterionic [2]Rotaxane with Intercomponent Ion Pairs[a]
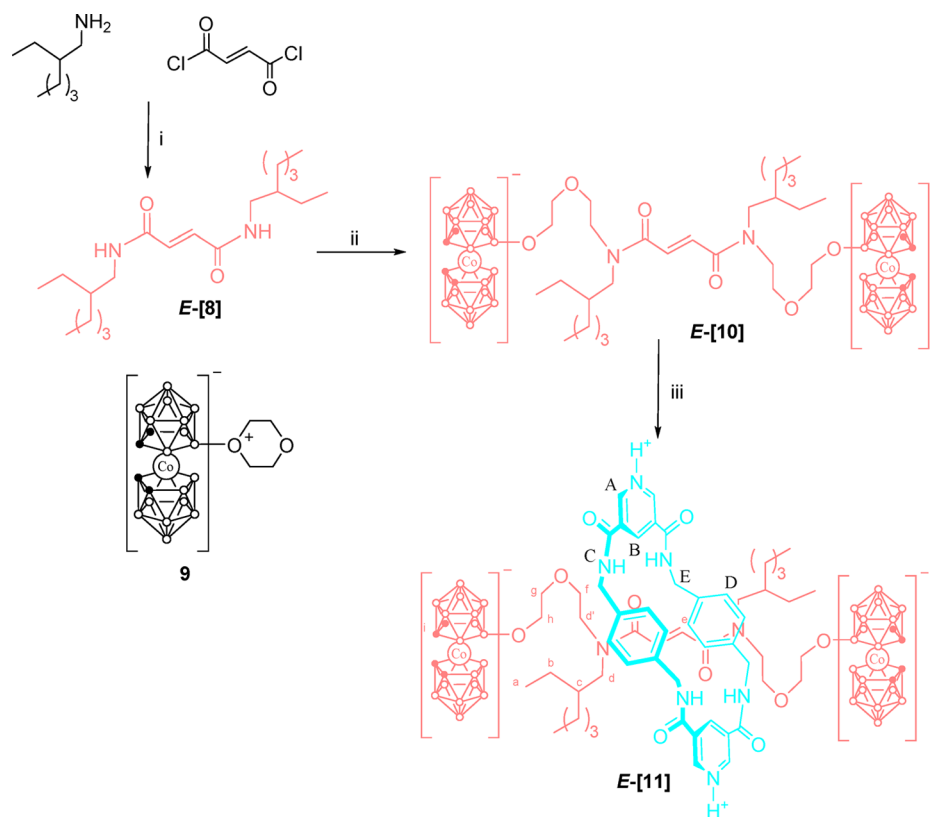
[a]Reagents and conditions: (i) Et_3N, $CHCl_3$, 0 °C, 2 h (42% yield). (ii) 1. NaH, toluene−tetrahydrofuran 2:1, 0 °C, 2 h. 2. [3,3′-Co(8-$C_4H_8O_2$-1,2-$C_2B_9H_{10}$)(1′,2′-$C_2B_9H_{11}$)] [9], rt, 18 h (90% yield). (iii) *Para*-xylene diamine, pyridine-3,5-dicarbonyl dichloride, Et_3N, $CHCl_3$, rt, 20 h. 2. 1 M $HCl_{(aq)}$ (18% yield).

interaction, also observed in the solid state, is responsible for the trans conformation of [2]⁻, which prevails in solution.[47]

Stuctures of the Salts in the Solid State. Single crystals suitable for investigation by X-ray crystallography were obtained by slow diffusion of hexane in a dimethyl sulfoxide solution of rotaxane *E*-[4]. The solid-state structure shows two sets of bifurcated hydrogen bonds between the amide groups of the macrocycle and the carbonyl groups of the fumaramide system. The crystal structure of *E*-[4] is typical (Figure 3) and shows the macrocycle in a chair conformation forming short, close-to-linear, hydrogen bonds orthogonal to the lone pairs of the fumaramide carbonyl groups. The O−HN distances are indicative of the strong H-bonding of the structure. Attempts to crystallize any of the protonated rotaxanes were unfruitful, and only *E*-[4] was obtained in some of the tests.

Dynamic Processes. The intramolecular dynamics were studied using the bidimensional nuclear magnetic resonance technique two-dimensional (2D) EXchange SpectroscopY (EXSY).[48] ¹H−¹H EXSY is based on the exchange rate between two nonequivalent hydrogen atoms that can exchange with one another conformationally or chemically. Selective irradiation of one resonance is followed, after a mixing time t_m, by detection of any perturbation, of resonances resulting from exchange processes.[49] It is a powerful tool to study multisite systems not amenable to study by conventional methods. Moreover, it gives site-to-site rate constants, whereas line-shape methods are sensitive only to lifetimes and are less informative. An alternative method already used in the study of dynamic processes is proton spin polarization transfer by selective

inversion recovery (SPT-SIR).[50] The use of this technique is recommended over variable-temperature (VT) NMR for many reasons including solvent viscosity changes over temperature, aggregation effects, or precipitation of the sample. However, EXSY is preferred over SPT-SIR when the dynamic processes are slow and the cross peaks are well-defined as it gives a fast and reliable quantitative measurement of the rate and allows calculation of the energy barriers. The equatorial and axial benzylic macrocycle protons (H_{E1} and H_{E2}) of fumaramide rotaxanes *E*-[4]−[7] are in slow conformational exchange due to the slow pirouetting motion of the macrocycle around the thread as can be observed by the broad appearance of the ¹H NMR signals (Figure 2).

EXSY experiments were performed in a 1:1 $CDCl_3$−CD_3CN mixture to overcome solubility problems. At room temperature, the exchange of the H_{E1} and H_{E2} protons is very slow in *E*-[4] due to the strong hydrogen bonding seen in the X-ray structure between the carbonyl groups on the thread and the amino hydrogen atoms on the macrocycle. EXSY measurements gave the room-temperature pseudo-first-order rate constant k_{obs} = 0.21 s⁻¹, which is equivalent to an activation free energy of 18.37 kcal mol⁻¹ (Table 1, entry 1; details of the kinetic measurements are given in the Supporting Information). Protonation of the pyridine groups on the macrocycle by any of the acids used in this study led to an increase of k_{obs}. This might be caused by electron reorganization in the macrocycle that weaken the hydrogen bonding in the molecule. Thus, protonation can be used to change the rate of pirouetting in this type of rotaxanes.
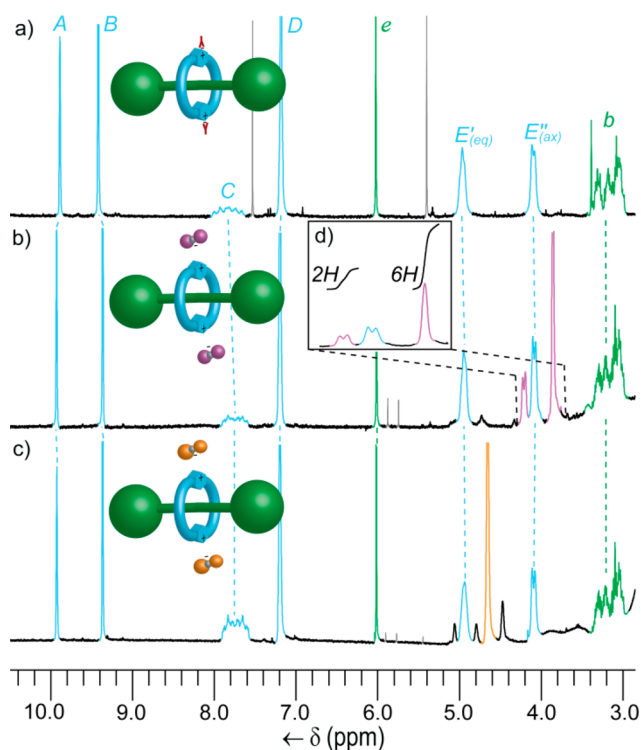
Figure 2. Partial ^{1}H NMR spectra (400 MHz, CD$_3$CN, 298 K) of protonated benzylic amide rotaxane with (a) TFA$^-$ counterion E-[**5**], (b) [3,3′−Co(1,2−C$_2$B$_9$H$_{11}$)$_2$]$^-$ counterion E-[**6**], (c) [8,8′,9,9′,12,12′−Br$_6$−3,3′−Co(1,2−C$_2$B$_9$H$_8$)$_2$]$^-$ counterion E-[**7**], and (d) expansion of the region showing the metallabisdicarbollide anion C$_C$−H resonances in rotaxane E-[**6**] with integrals. The lettering corresponds to that shown in Scheme 1
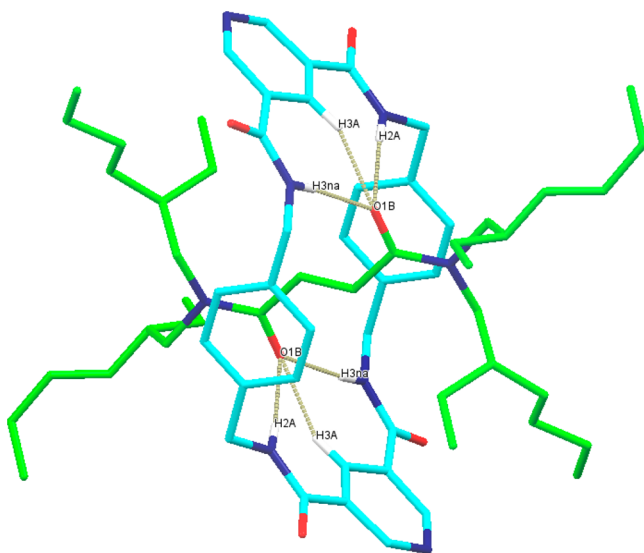

Figure 3. X-ray crystal structure of rotaxane E-[**4**] (for clarity, carbon atoms of the macrocycle are shown in blue, and the carbon atoms of the thread are shown in green; oxygen atoms are depicted in red, nitrogen atoms are dark blue, and selected hydrogen atoms are white. Disorder has been also omitted). Intramolecular hydrogen bond distances (Å): O1B−H2A = 2.16, O1B−H3na = 2.14, O1B−H3A = 2.15.

Comparing the conformational exchange rates of E-[**5**]−[**7**] (Table 1, entries 2, 4, and 6) it is apparent that rotaxanes with WCAs, namely, E-[**6**] and E-[**7**], undergo more rapid

pirouetting than E-[**5**] with closely coordinating trifluoroacetate anions. This experimental evidence is what we were expecting: the boron cluster containing rotaxanes show higher k_{obs} and lower energy barrier than E-[**5**] because the ion pair interaction of the anions with the pyridinium protons is weaker. The WCA nature of boron clusters allows a higher degree of freedom to the rotation of the macrocycle. Interestingly, it can be observed that there are some differences between E-[**6**] and E-[**7**]. The presence of B−Br vertices in E-[**7**] causes a higher acidity on the C$_C$-H hydrogen atoms seen by their downfield shift in the ^{1}H NMR. This could be the reason for a lower interaction between the metallabisdicarbollide and the macrocycle in E-[**7**], which causes a higher k_{obs}, 45.6 for E-[**7**] versus 40.3 s^{-1} for E-[**6**]. The exchange rates correspond to activation energies ($\Delta G^{\ddagger}$) of around 15 kcal mol^{-1}, and the difference in energy between the least and the most coordinating anion is 0.5 kcal mol^{-1}. This energy difference is small compared to the 3.2 kcal mol^{-1} energy barrier found upon protonation. Moreover, it is even smaller compared to the barrier found on similar systems upon photoisomerization of the thread component (6.8 kcal mol^{-1}).[12] The presence of a fumaryl group in the thread of compounds E-[**5**]−[**7**] gives the opportunity to study the dynamics of their isomerized Z counterparts upon UV light. Irradiation of E-[**4**] at 312 nm gives Z-[**4**] in 59% yield. Protonation of Z-[**4**] gave the desired Z-[**5**]−[**7**] rotaxanes. Characterization of Z isomers can be found in the Supporting Information. Preliminary NMR experiments on photoisomerized Z-[**5**], Z-[**6**], and Z-[**7**] show that counteranion effects are negligible in these rotaxanes where the pirouetting rate is very high (on the order of 1 s^{-1} for similar systems). As an example, the ^{1}H NMR spectrum of Z-[**5**] at 223 K shows a single peak corresponding to the axial and equatorial H$_D$ hydrogen atoms on the macrocycle, indicating a very fast rotation. Therefore, we propose that the use of different counteranions could play a key role on the fine-tuning of pirouetting motion at slow dynamics.

It is known that solvent effect or moisture can change the dynamics in interlocked molecules.[50] As we are seeking for a fine-tuning of the motion we wanted to check that the addition of a solvent would not change the trend observed before upon using WCA. Moisture effects have been discarded as all experiments were carried out under dry conditions. In our case we would like to study the effect upon addition of methanol to the mixture chloroform/acetonitrile that we were already using. As discussed above, the slow pirouetting motion is attributed to the fact that the fumaryl template forms strong interactions with the macrocycle, causing a decrease on the effect of the counteranion. The addition of a polar solvent such as methanol could break hydrogen bonding and increase the kinetic constants. However, counteranions could play an additional role by protecting the hydrogen bonding from solvent effects. To demonstrate this hypothesis we repeated 2D EXSY experiments adding 30% of CD$_3$OD to the solvent mixture. Indeed, a very small difference in k_{obs}, 19.75 versus 19.28 s^{-1}, was observed for E-[**5**]. In the case for E-[**6**], the increase in k_{obs} was more pronounced although it stayed within the same order of magnitude, 40.3 and 61.4 s^{-1}, respectively. Overall, it was shown that the use of WCA as counteranions increase the pirouetting rate in positively charged rotaxanes.

Zwitterion E-[11]. EXSY experiments on E-[**11**] give a k_{obs} of 24.2 s^{-1} and an energy barrier of 15.5 kcal mol^{-1}. The structure of E-[**11**] prevents a close ion pair between the negative and the positive charges as the first is located on the macrocycle and the latter on the stoppers. To keep the

Table 1. k and $\Delta G^{\ddagger}$ Values for Compounds E-[4]–[7] and E-[11] Calculated by the 2D-EXSY Technique

entry	rotaxane	solvent	$k_{obs}{}^{a}$ (s^{-1})	$\Delta G^{\ddagger}_{298}{}^{a}$ (kcal mol^{-1})
1	E-[4]	1:1 CDCl$_3$–CD$_3$CN	0.21	18.37
2	E-[5]	1:1 CDCl$_3$–CD$_3$CN	19.75	15.67
3	E-[5]	35:35:30 CDCl$_3$–CD$_3$CN–CD$_3$OD	19.28	15.68
4	E-[6]	1:1 CDCl$_3$–CD$_3$CN	40.33	15.25
5	E-[6]	35:35:30 CDCl$_3$–CD$_3$CN–CD$_3$OD	61.38	14.99
6	E-[7]	1:1 CDCl$_3$–CD$_3$CN	45.59	15.17
7	E-[11]	1:1 CDCl$_3$–CD$_3$CN	24.25	15.54

^{a}Dynamic constants calculated at room temperature (298 K).

electrostatic force between ions, the macrocycle or the thread should distort from their structure. Therefore, the motion will be hindered, and the intramolecular electrostatic interactions will slow down the kinetics. Indeed, a comparison between k_{obs} of E-[11] and E-[6] shows that the latter rotates twice as fast. In addition to this, E-[11] contains cobaltabisdicarbollide moieties that behave as both a stopper and an electroactive unit. Its incorporation into these potentially machinelike structures could give rise to a series of electrochemically induced events such as electron transfer, acting in the sense of *para*-carborane or C$_{60}$ in a new kind of electroactive dyad.[51,52] However, we wanted to see if its redox and optical properties changed because of the intramolecular interactions present in the molecule. Interestingly, spectroscopic and electrochemical properties of the cobaltabisdicarbollide are not affected by its integration in the rotaxane skeleton (see Supporting Information for full details).

CONCLUSIONS

In conclusion, we have demonstrated that the dynamics of positively charged rotaxanes can be fine-tuned by using different counterions. The rate of pirouetting follows the expected trend of E-[5] < E-[6] < E-[7], the latter being the fastest to rotate since hexabromo derivative of cobaltabisdicarbollide is the weakest coordinating anion. The difference in the rotation frequency between them is within the same order of magnitude, and therefore, a proper modulation of the pirouetting motion is achievable by this methodology. The effect of the counteranion is important under slow kinetics but is negligible when the pirouetting rate is very high, as in the case for Z isomers. On the other hand, the pirouetting rate in E-[11] is twice as slow as E-[6], where intramolecular electrostatic interactions play a key role. This indicates that cobaltabisdicarbollide stoppers are slowing down the rotation of the macrocycle by their interactions with the protonated pyridine groups. Besides, E-[11] is an interesting example of a zwitterionic rotaxane, and investigations on the use of its redox properties as an additional stimulus to control rotaxane dynamics are currently under way in our laboratories.

ASSOCIATED CONTENT

S **Supporting Information**

EXSY experimental details are fully explained. Spectroscopic and electrochemical data for E-[11] is shown. Crystallographic data for E-[4]. This material is available free of charge via the Internet at http://pubs.acs.org.

AUTHOR INFORMATION

Corresponding Authors
*E-mail: pau.farras@ncl.ac.uk. (P.F.)
*E-mail: teixidor@icmab.es. (F.T.)

REFERENCES

(1) Sauvage, J.-P.; Dietrich-Buchecker, C. *Molecular Catenanes, Rotaxanes and Knots: A Journey through the World of Molecular Topology*; John Wiley & Sons: New York, NY, 2008.
(2) Browne, W. R.; Feringa, B. L. *Nat. Nanotechnol.* **2006**, *1*, 25−35.
(3) Rescifina, A.; Zagni, C.; Iannazzo, D.; Merino, P. *Curr. Org. Chem.* **2009**, *13*, 448−481.
(4) Raehm, L.; Kern, J.-M.; Sauvage, J.-P. *Chem.—Eur. J.* **1999**, *5*, 3310−3317.
(5) Hirose, K.; Ishibashi, K.; Shiba, Y.; Doi, I.; Tobe, Y. *Chem.—Eur. J.* **2008**, *14*, 5803−5811.
(6) Kay, E. R.; Leigh, D. A.; Zerbetto, F. *Angew. Chem., Int. Ed.* **2007**, *46*, 72−191.
(7) Badjic, J. D.; Balzani, V.; Credi, A.; Silvi, S.; Stoddart, J. F. *Science* **2004**, *303*, 1845−1849.
(8) Brouwer, A. M.; Frochot, C.; Gatti, F.; Leigh, D. A.; Mottier, L.; Paolucci, F.; Roffia, S.; Wurpel, G. W. H. *Science* **2001**, *291*, 2124−2128.
(9) Balzani, V.; Clemente-Leon, M.; Credi, A.; Ferrer, B.; Venturi, M.; Flood, A. H.; Stoddart, J. F. *Proc. Natl. Acad. Sci. U.S.A.* **2006**, *103*, 1178−1183.
(10) Periyasamy, G.; Sour, A.; Collin, J. P.; Sauvage, J. P.; Remacle, F. *J. Phys. Chem. B* **2009**, *113*, 6219−6229.
(11) Bermudez, V.; Capron, N.; Gase, T.; Gatti, F. G.; Kajzar, F.; Leigh, D. A.; Zerbetto, F.; Zhang, S. *Nature* **2000**, *406*, 608−611.
(12) Gatti, F. G.; Leon, S.; Wong, J. K. Y.; Bottari, G.; Altieri, A.; Farran-Morales, M. A.; Teat, S. J.; Frochot, C.; Leigh, D. A.; Brouwer, A. M.; Zerbetto, F. *Proc. Natl. Acad. Sci. U.S.A.* **2003**, *100*, 10−14.
(13) Grimes, R. N. *J. Chem. Educ.* **2004**, *81*, 658−672.
(14) Reed, C. A.; Kim, K. C.; Bolskar, R. D.; Mueller, L. J. *Science* **2000**, *289*, 101−104.
(15) Masalles, C.; Llop, J.; Viñas, C.; Teixidor, F. *Adv. Mater.* **2002**, *14*, 826−829.
(16) Farras, P.; Juarez-Perez, E. J.; Lepsik, M.; Luque, R.; Nunez, R.; Teixidor, F. *Chem. Soc. Rev.* **2012**, *41*, 3445−3463 and references therein.
(17) Blanch, R. J.; Williams, M.; Fallon, G. D.; Gardiner, M. G.; Kaddour, R.; Raston, C. L. *Angew. Chem., Int. Ed.* **1997**, *36*, 504−506.

(18) Giner-Planas, J.; Viñas, C.; Teixidor, F.; Comas-Vives, A.; Ujaque, G.; Lledós, A.; Light, M. E.; Hursthouse, M. B. *J. Am. Chem. Soc.* **2005**, *127*, 15976−15982.

(19) Masalles, C.; Borros, S.; Viñas, C.; Teixidor, F. *Adv. Mater.* **2000**, *12*, 1199−1202.

(20) Cígler, P.; Kožíšek, M.; Řezáčová, P.; Brynda, J.; Otwinowski, Z.; Pokorná, J.; Plešek, J.; Grüner, B.; Dolečková-Marešová, L.; Máša, M.; Sedláček, J.; Bodem, J.; Kräusslich, H.-G.; Král, V.; Konvalinka, J. *Proc. Natl. Acad. Sci. U.S.A.* **2005**, *102*, 15394−15399.

(21) Stoica, A. I.; Viñas, C.; Teixidor, F. *Chem. Commun.* **2008**, 6492−6494.

(22) Stoica, A. I.; Viñas, C.; Teixidor, F. *Chem. Commun.* **2009**, 4988−4990.

(23) Chu, P. L. E.; Wang, L. Y.; Khatua, S.; Kolomeisky, A. B.; Link, S.; Tour, J. M. *ACS Nano* **2012**, *7*, 35−41.

(24) Vives, G.; Tour, J. M. *Acc. Chem. Res.* **2009**, *42*, 473−487.

(25) Hawthorne, M. F.; Zink, J. I.; Skelton, J. M.; Bayer, M. J.; Liu, C.; Livshits, E.; Baer, R.; Neuhauser, D. *Science* **2004**, *303*, 1849−1851.

(26) Kennedy, R. D.; Knobler, C. B.; Hawthorne, M. F. *Inorg. Chem.* **2009**, *48*, 9377−9384.

(27) Farràs, P.; Viñas, C.; Teixidor, F. *J. Organomet. Chem.* **2013**, *747*, 119−125.

(28) Gatti, F. G.; Leigh, D. A.; Nepogodiev, S. A.; Slawin, A. M. Z.; Teat, S. J.; Wong, J. K. Y. *J. Am. Chem. Soc.* **2001**, *123*, 5983−5989.

(29) Laursen, B. W.; Nygaard, S.; Jeppesen, J. O.; Stoddart, J. F. *Org. Lett.* **2004**, *6*, 4167−4170.

(30) Matel, L.; Macásek, F.; Rajec, P.; Hermánek, S.; Plešek, J. *Polyhedron* **1982**, *1*, 511−519.

(31) Rojo, I.; Pedrajas, J.; Teixidor, F.; Viñas, C.; Kivekas, R.; Sillanpaä, R.; Sivaev, I.; Bregadze, V.; Sjöberg, S. *Organometallics* **2003**, *22*, 3414−3423.

(32) *APEX II versions v1.0 −22, v2009.1−0 and v2009.1−02*; Bruker AXS Inc.: Madison, WI, USA, 2007.

(33) *SAINT versions V.2.10, 2003, V/.60 A and V7.60 A*; Bruker AXS Inc.: Madison, WI, USA, 2007.

(34) Sheldrick, G. M. *Acta Crystallogr., Sect. A* **2008**, *64*, 112 −122.

(35) TWINABS Version 2008/4 Bruker AXS; Blessing *Acta Crystallogr.* **1995**, *A51*, 33−38.

(36) Burla, M. C.; Caliandro, R.; Camalli, M.; Carrozzini, B.; Cascarano, G. L.; Giacovazzo, C.; Mallamo, M.; Mazzone, A.; Polidori, G.; Spagna, R. *J. Appl. Crystallogr.* **2012**, *45*, 357−361.

(37) Alvarez-Pérez, M.; Goldup, S. M.; Leigh, D. A.; Slawin, A. M. Z. *J. Am. Chem. Soc.* **2008**, *130*, 1836−1838.

(38) Mateo-Alonso, A.; Prato, M. *Tetrahedron* **2006**, *62*, 2003−2007.

(39) An analogous rotaxane with aryl stoppers was also synthesized; however, the solubility of the protonated compounds was very poor in chlorinated solvents and in a 1:1 mixture of $CDCl_3/CD_3CN$ used to perform 2D-NMR measurements.

(40) Langton, M. J.; Beer, P. D. *Acc. Chem. Res.* **2014**, DOI: 10.1021/ar500012a.

(41) Spence, G. T.; Serpell, C. J.; Sardinha, J.; Costa, P. J.; Félix, V.; Beer, P. D. *Chem.—Eur. J.* **2011**, *17*, 12955−12966.

(42) Davidson, G. J.; Loeb, S. J.; Parekh, N. A.; Wisner, J. A. *J. Chem. Soc., Dalton Trans.* **2001**, 3135−3136.

(43) Isnin, R.; Kaifer, A. E. *J. Am. Chem. Soc.* **1991**, *113*, 8188−8190.

(44) Barrell, M. J.; Leigh, D. A.; Lusby, P. J.; Slawin, A. M. *Angew. Chem., Int. Ed.* **2008**, *47*, 8036−8039.

(45) Lestini, E.; Nikitin, K.; Stolarczyk, J. K.; Fitzmaurice, D. *ChemPhysChem* **2012**, *13*, 797−810.

(46) Hardie, M. J.; Raston, C. L. *Chem. Commun.* **2001**, 905−906.

(47) On May 20th 2014, seven crystal structures that contain 8,8′-Br_2-COSAN were detected at the Cambridge Data Base. In all of them the conformation is *trans*. Particularly for this work the structure PUCWEQ Kazheva, O.; Alexandrov, G.; Kravchenko, A.; Starodub, V.; Lobanova, I.; Sivaev, I.; Bregadze, V.; Buravov, L.; Dyachenko, O. *Solid State Sci.* **2008**, *10*, 1734−39.

(48) Wynants, C.; van Binst, G.; Miigge, C.; Jurkschat, K.; Tzschach, A.; Pepermans, H.; Gielen, M.; Willem, R. *Organometallics* **1985**, *4*, 1906−1909.

(49) Perrin, C. L.; Dwyer, T. J. *Chem. Rev.* **1990**, *90*, 935−967.

(50) Leigh, D. A.; Murphy, A.; Smart, J. P.; Deleuze, M. S.; Zerbetto, F. *J. Am. Chem. Soc.* **1998**, *120*, 6458−6467.

(51) Ghirotti, M.; Schwab, P. F. H.; Indelli, M. T.; Chiorboli, C.; Scandola, F. *Inorg. Chem.* **2006**, *45*, 4331−4333.

(52) Scarel, F.; Valenti, G.; Gaikwad, S.; Marcaccio, M.; Paolucci, F.; Mateo-Alonso, A. *Chem.—Eur. J.* **2012**, *18*, 14063−14068.